Available online at www.sciencedirect.com
SCIENCE DIRECT
Journal of Power Sources 146 (2005) 598–601
JOURNAL OF POWER SOURCES
www.elsevier.com/locate/jpowsour

Synthesis of $(1-2x)LiNi_{1/2}Mn_{1/2}O_2 \cdot xLi[Li_{1/3}Mn_{2/3}]O_2 \cdot xLiCoO_2$ $(0 \leq x \leq 0.5)$ electrode materials and comparative study on cooling rate

Lianqi Zhang [a], Kazunori Takada [a,b,*], Narumi Ohta [a], Katsutoshi Fukuda [a], Takayoshi Sasaki [a,b]

[a] *Advanced Materials Laboratory, National Institute for Materials Science, Namiki 1-1, Tsukuba, Ibaraki 305-0044, Japan*
[b] *CREST, Japan Science and Technology Agency (JST), Japan*

Available online 25 April 2005

Abstract

Layered cathode materials with the nominal compositions of $(1-2x)LiNi_{1/2}Mn_{1/2}O_2 \cdot xLi[Li_{1/3}Mn_{2/3}]O_2 \cdot xLiCoO_2$ $(0 \leq x \leq 0.5)$ were synthesized by a simple solid-state reaction on the basis of good structural compatibility between the three layered compounds, $LiNi_{1/2}Mn_{1/2}O_2$, $Li[Li_{1/3}Mn_{2/3}]O_2$, and $LiCoO_2$. Increasing contents of $Li[Li_{1/3}Mn_{2/3}]O_2$ and $LiCoO_2$ in the materials decreased the occupancy of transitional metal ions in Li layers and thus remarkably improved electrochemical performances; but it also brought about an irreversible initial charge plateau when x reached 0.3. The comparative studies on cooling rates showed that different cooling rates in the material preparation hardly gave different electrode performances.

Keywords: Lithium ion battery; Layered cathode; Lithium cobalt nickel manganese oxides; Solid-state reaction; Cooling rate

1. Introduction

In the search for an improved cathode material, the materials in two series with the performances comparable to or better than those of $LiCoO_2$ recently attracted intense attention. One is layered $LiCo_{1-2x}Ni_xMn_xO_2$ $(0 \leq x \leq 0.5)$ [1–3], which can be alternatively written as $2xLiNi_{1/2}Mn_{1/2}O_2 \cdot (1-2x)LiCoO_2$ in composite notation; the other is layered $Li[Ni_xLi_{1/3-2x/3}Mn_{2/3-x/3}]O_2$ $(0 \leq x \leq 0.5)$ [4–6], which can be rewritten as $2xLiNi_{1/2}Mn_{1/2}O_2 \cdot (1-2x)Li[Li_{1/3}Mn_{2/3}]O_2$. It can be believed that the success in preparing the two series of materials is based on the good structural comparability between $LiNi_{1/2}Mn_{1/2}O_2$ and $LiCoO_2$ as well as between $LiNi_{1/2}Mn_{1/2}O_2$ and $Li[Li_{1/3}Mn_{2/3}]O_2$. In addition, the earlier reports on the system of $LiCoO_2$-$Li[Li_{1/3}Mn_{2/3}]O_2$ also evidenced the strong ability of structural mergence (or integration) between $LiCoO_2$ and $Li[Li_{1/3}Mn_{2/3}]O_2$ [7,8]. We recently demonstrated that the new layered cathode materials in the system of $(1\text{-}x\text{-}y)LiNi_{1/2}Mn_{1/2}O_2 \cdot xLi[Li_{1/3}Mn_{2/3}]O_2 \cdot yLiCoO_2$ can be also prepared on the basis of good structural compatibility between three layered compounds, $LiNi_{1/2}Mn_{1/2}O_2$, $Li[Li_{1/3}Mn_{2/3}]O_2$ and $LiCoO_2$ [9].

Both rapid and slow coolings were adopted to prepare these materials in the references [1–12]. Different cooling rate in the preparation of these materials can bring about some differences in structure [12] and valence states of cations accompanying different degree of oxygen defect in materials, finally resulting in the differences in performances. Dahn and co-workers reported that slightly higher capacities were achieved by quenching method than by furnace cooling (slow cooling) for several samples in the series of $2xLiNi_{1/2}Mn_{1/2}O_2 \cdot (1-2x)Li[Li_{1/3}Mn_{2/3}]O_2$ $(0 \leq x \leq 0.5)$ [6]; nevertheless, Kang and Amine reported significant effects of cooling rate on structure and electrochemistry in $0.5LiNi_{1/2}Mn_{1/2}O_2 \cdot 0.5Li[Li_{1/3}Mn_{2/3}]O_2$ [12].

In this work, layered cathode materials with the nominal compositions of $(1-2x)LiNi_{1/2}Mn_{1/2}O_2 \cdot xLi[Li_{1/3}Mn_{2/3}]O_2 \cdot xLiCoO_2$ $(0 \leq x \leq 0.5)$, which can be also written

* Corresponding author. Tel.: +81 29 860 4317; fax: +81 29 854 9061.
E-mail address: takada.kazunori@nims.go.jp (K. Takada).

0378-7753/$ – see front matter © 2005 Elsevier B.V. All rights reserved.
doi:10.1016/j.jpowsour.2005.03.122

as $Li[Li_{x/3}Ni_{(1-2x)/2}Mn_{(3-2x)/6}Co_x]O_2$ $(0 \le x \le 0.5)$ in layered notation, were synthesized via a simple solid state reaction under the different cooling rates (quenching and furnace cooling). The structure and electrochemical performances were comparatively examined.

2. Experimental

Materials were prepared by a conventional solid-state reaction using acetates as starting materials. A stoichiometric ratio of $Ni(CH_3COO)_2{\cdot}4H_2O$, $Mn(CH_3COO)_2{\cdot}4H_2O$, $Co(CH_3COO)_2{\cdot}4H_2O$ and $LiCH_3COO{\cdot}2H_2O$ were mixed and ground using a mortar and a pestle. The mixture was decomposed at 450 °C in air and ground after cooling. The decomposed mixture was pelletized into a 3 mm thick tablet at 200 kg cm^{-2}. The pellet was calcined at 1000 °C in air for 4 h and then quenched in liquid nitrogen or subjected to furnace cooling. Finally, the pellet was ground and kept in a desiccator with blue silica-gel.

The crystal structures of samples were investigated by powder X-ray diffraction (XRD). XRD data were collected on a diffractometer (RINT2200, Rigaku) with graphite-monochromatic Cu Kα radiation (λ = 0.15406 nm). For Rietveld refinement, the XRD data were collected in the 2θ range of 10–120° with a step of 0.02° and a constant counting time of 10 s. Structure parameters were refined by a Rietveld method using a computer program (RIETAN-2000) [13] on the basis of α-$NaFeO_2$-type structure with space group *R*-3*m*. A virtual chemical species representing the transition metal elements in samples, M, was used in the refinement. It has the mean scattering amplitude of the transition metal elements calculated from the chemical composition. Li, M and O were distributed to 3*a* (0, 0, 0), 3*b* (0, 0, 1/2) and 6c (0, 0, *z*) sites, respectively; and the total occupancies of each site were constrained to be unity.

The charge and discharge characteristics of Li–Ni–Co–Mn–O cathodes were examined in coin-type half-cells (Li/Li–Ni–Co–Mn–O). Cells were composed of a cathode and a lithium metal anode (Honjou Kinzoku Co., Japan) separated by a porous polypropylene film (Celgard 3401) and two glass fiber mats. The cathode consisted of 20 mg active material and 12 mg conductive binder [8 mg polytetrafluoroethylene (PTFE) and 4 mg acetylene black]. It was pressed on a titanium mesh at 300 kg cm^{-2} and then dried under vacuum at 120 °C for 12 h. The electrolyte solution was a 1:1 mixture of ethylene carbonate (EC) and diethylcarbonate (DEC) containing 1 M $LiPF_6$. All cells were assembled in an argon-filled dry box. Cells were cycled in the voltage range of 2.5–4.6 V at a constant current density of 20 mA g^{-1} (0.23 mA cm^{-2}) at 25 °C.

3. Results and discussion

Fig. 1 shows the XRD patterns of $(1-2x)LiNi_{1/2}Mn_{1/2}O_2{\cdot}xLi[Li_{1/3}Mn_{2/3}]O_2{\cdot}xLiCoO_2$ $(0 \le x \le 0.5)$ pre-

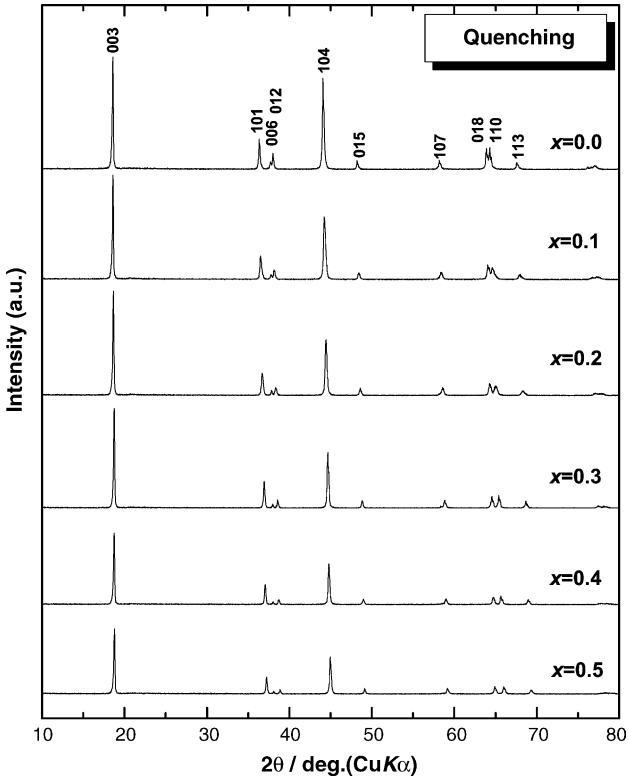

Fig. 1. XRD patterns of $(1-2x)$ $LiNi_{1/2}Mn_{1/2}O_2{\cdot}xLi[Li_{1/3}Mn_{2/3}]O_2{\cdot}xLiCoO_2$ $(0 \le x \le 0.5)$ prepared by quenching method.

pared by the quenching method. All reflections were indexable based on a layered α-$NaFeO_2$-type structure (space group *R*-3*m*, no. 166). The series of the samples prepared by furnace cooling gave the similar XRD patterns to the quenched ones. The changes in hexagonal lattice constants and occupancy of transitional metal ions in Li layers are illuminated in Fig. 2. The lattice parameters, *a* and *c*, continuously decreased with increasing *x* value. Correspondingly, the volume of unit cell also presented monotonous decrease. The *a* in hexagonal unit cell is a measure of the average M–M (M = Li, Ni, Co, Mn) distance in slabs, the layers filled predominantly by transitional metal ions; while *c* is the thickness of three slabs and three interslabs (Li layers) [14,15]. According to reports [1–6], the valence states of Ni, Co and Mn in these materials investigated in this work can be assumed to have 2+, 3+ and 4+, respectively. The series of $(1-2x)LiNi_{1/2}Mn_{1/2}O_2{\cdot}xLi[Li_{1/3}Mn_{2/3}]O_2{\cdot}xLiCoO_2$ $(0 \le x \le 0.5)$ had a substitution equation: $3Ni^{2+} + Mn^{4+} = Li^+ + 3Co^{3+}$. The ionic radii of Li^+, Ni^{2+}, Co^{3+} and Mn^{4+} are 0.76, 0.69, 0.53 and 0.54 Å, respectively [16]; therefore, the average ionic radius of $[Li^+ + 3Co^{3+}]$ is smaller than that of $[3Ni^{2+} + Mn^{4+}]$ (0.59 and 0.65 Å, respectively). The smaller mean ionic radius will cause shrinkage of the transitional metal layers, resulting in the shrinkage in *a* and *c* axes with increasing *x*. The cooling rate affected lattice parameters little. Rietveld refinements showed that the occupancy of transitional metal ions in Li layers for the

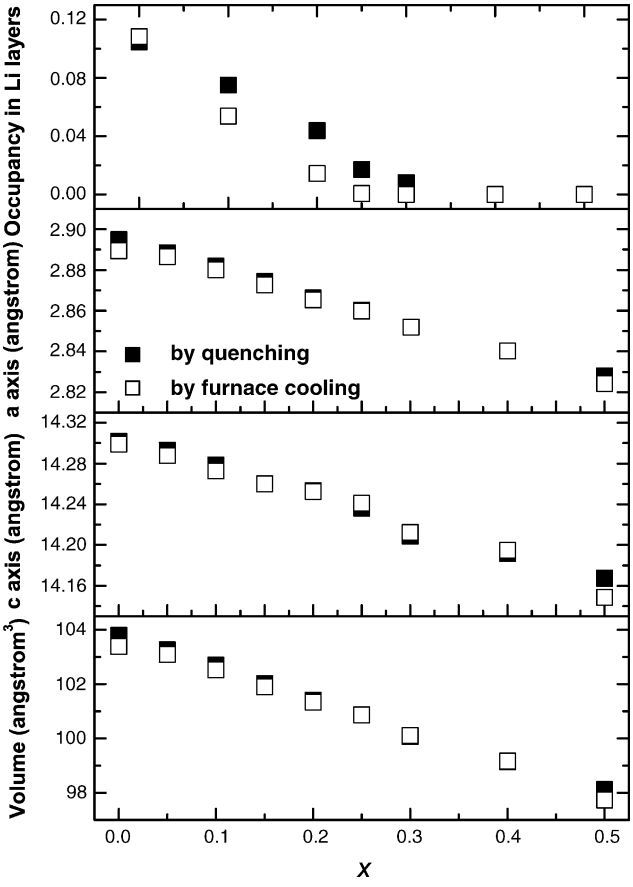

Fig. 2. Lattice constants, unit cell volume and occupancy of transitional metal ions in Li layers for $(1-2x)LiNi_{1/2}Mn_{1/2}O_2{\cdot}xLi[Li_{1/3}Mn_{2/3}]O_2{\cdot}xLiCoO_2$ $(0 \le x \le 0.5)$ in hexagonal unit cell.

samples prepared by quenching method gradually decreased with increasing x value; degree of such cation mixing was very small for the samples with $x = 0.4$ and 0.5. The furnace cooling can reduce occupancy of transitional metal ions in Li layers with the exception of $x = 0$ and it was already unobservable in the cases of $x \ge 0.25$.

Fig. 3 shows the initial charge–discharge curves of $(1-2x)LiNi_{1/2}Mn_{1/2}O_2{\cdot}xLi[Li_{1/3}Mn_{2/3}]O_2{\cdot}xLiCoO_2$ $(0 \le x \le 0.5)$ prepared by both quenching and furnace cooling. Initial charge–discharge capacities gradually increased with increasing x, and irreversible capacity also gradually increased, as shown in Fig. 4. In the figure, one theoretical capacity line was also drawn on the basis of the assumption: all transitional metals were oxidized to 4+ in oxidation state, because Ni, Co, and Mn ions in layered structures are, in general, oxidized to tetravalent states in lithium batteries. However, initial charge capacities of the samples with $0.25 \le x \le 0.5$ and initial discharge capacities for $0.4 \le x \le 0.5$ exceeded the theoretical capacity line. Such an anomaly large capacity was also observed in $Li[Ni_xLi_{1/3-2x/3}Mn_{2/3-x/3}]O_2$ by Lu et al. [4–6]. They attributed the excess initial charge capacity over that corresponding to the oxidization of transitional metal ions to 4+ to simultaneous removal of Li^+ and oxygen at about 4.5 V, which took place only in the first charge process with a clear

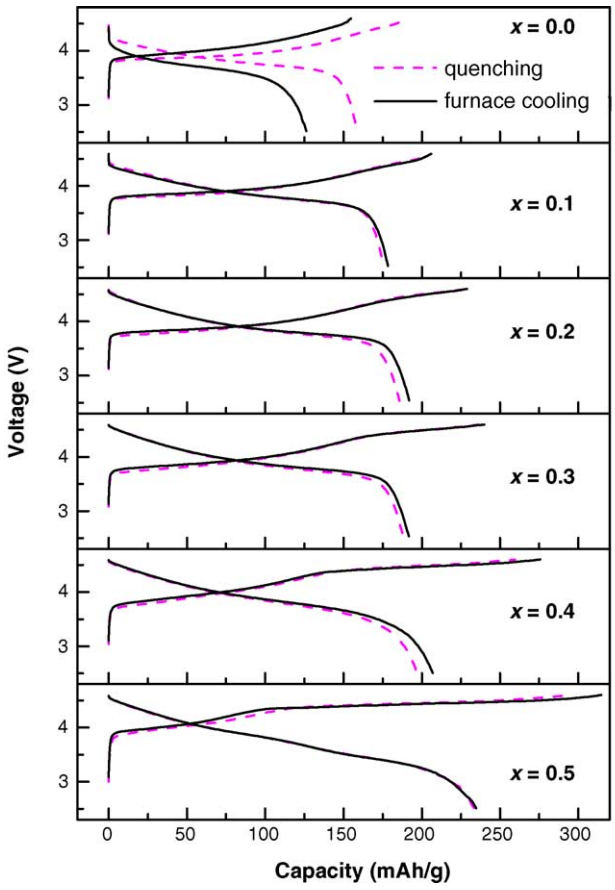

Fig. 3. Initial charge–discharge curves of $(1-2x)LiNi_{1/2}Mn_{1/2}O_2{\cdot}xLi[Li_{1/3}Mn_{2/3}]O_2{\cdot}xLiCoO_2$ $(0 \le x \le 0.5)$ galvanostatically cycled in the voltage range of 4.6–2.5 V at a constant current density of 20 mA g^{-1} (0.23 mA cm^{-2}) at 25 °C.

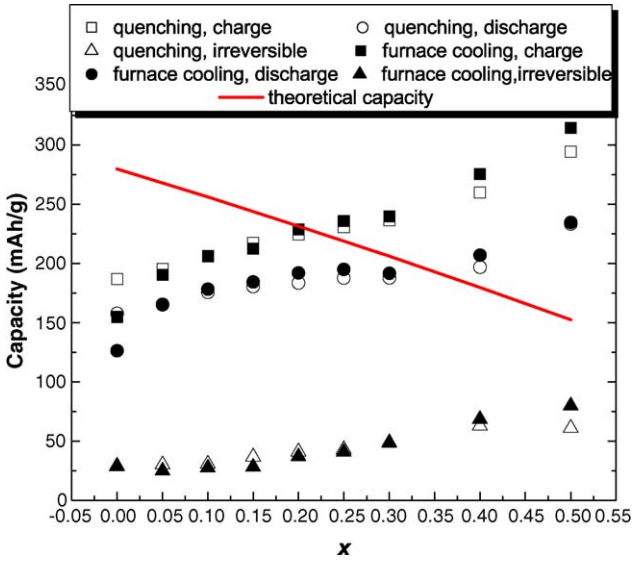

Fig. 4. Initial charge, discharge and irreversible capacities for $(1-2x)LiNi_{1/2}Mn_{1/2}O_2{\cdot}xLi[Li_{1/3}Mn_{2/3}]O_2{\cdot}xLiCoO_2$ $(0 \le x \le 0.5)$ as well as its theoretical capacity line. The theoretical capacity was calculated assuming all transitional metals were oxidized to 4+ in oxidation state.

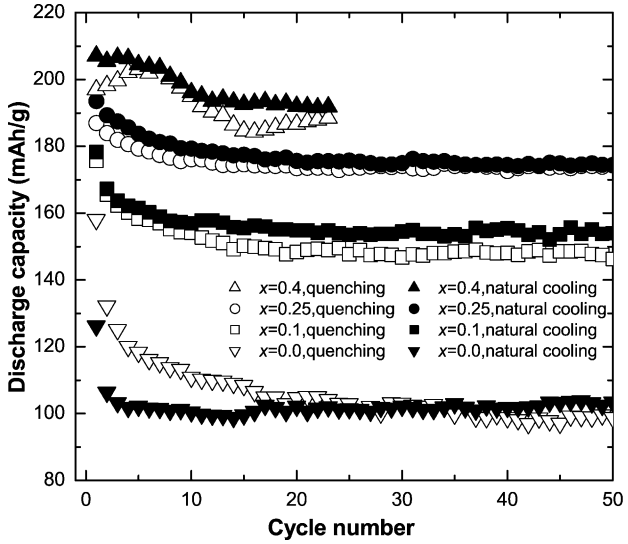

Fig. 5. Cycling performance of several typical samples in $(1-2x)LiNi_{1/2}Mn_{1/2}O_2{\cdot}xLi[Li_{1/3}Mn_{2/3}]O_2{\cdot}xLiCoO_2$ $(0 \le x \le 0.5)$.

irreversible potential plateau. Such irreversible plateaus were also observed clearly for our samples and developed with increasing x. Therefore, similar abnormal oxidation process will be the reason for the increasing capacity with increasing x.

When the abnormal oxidation process takes place, the capacity is limited not by the amount of transition metal ions in the slabs but by the amount of lithium ions in the interslabs. The structure analysis showed that increasing x decreased the occupancy of the transition metal ions in the interslabs; that is, it increased the amount of lithium ions in the interslabs, which is considered to increase the capacity to some extent.

The furnace-cooled samples showed nearly the same or slightly high capacity except for $x = 0$ in comparison with those obtained by the quenching method, which is different from the results reported for $2xLiNi_{1/2}Mn_{1/2}O_2{\cdot}(1-2x)Li[Li_{1/3}Mn_{2/3}]O_2$ $(0 \le x \le 0.5)$. Smaller capacities were observed in the furnace-cooled or slowly-cooled samples compared with the quenched samples [6,12], which may be because single-phase samples were not obtained when they were slowly cooled [12]. In fact, all the samples in the present study were single-phase, and the different cooling methods did not result in different capacity.

The cycling performance for several typical samples is shown in Fig. 5. The samples with $x \ge 0.2$ maintained the discharge capacities larger than 170 mAh g^{-1} and are promising materials. The samples prepared by furnace cooling showed similar cycleability to those prepared by quenching method except for $x = 0$.

4. Conclusion

Layered cathode materials with the nominal compositions of $(1-2x)LiNi_{1/2}Mn_{1/2}O_2{\cdot}xLi[Li_{1/3}Mn_{2/3}]O_2{\cdot}xLiCoO_2$ $(0 \le x \le 0.5)$ were successfully prepared by conventional solid-state reaction. Their XRD patterns identified that all materials were pure phases with layered structure, indicating good structural compatibility between three layered compounds, $LiNi_{1/2}Mn_{1/2}O_2$, $Li[Li_{1/3}Mn_{2/3}]O_2$ and $LiCoO_2$. The capacity gradually increased with increasing contents of $Li[Li_{1/3}Mn_{2/3}]O_2$ and $LiCoO_2$ in the materials, which was ascribed to decreasing occupancy of transitional metal ions in Li layers and developing unusual oxidation process similar to that observed for $2xLiNi_{1/2}Mn_{1/2}O_2{\cdot}(1-2x)Li[Li_{1/3}Mn_{2/3}]O_2$. The samples with $x \ge 0.2$ can deliver a reversible capacity more than 190 mAh g^{-1}. The samples synthesized by different cooling rates showed similar characteristics.

Acknowledgements

This work was partially funded by Ministry of Economy, Trade and Industry (METI) and New Energy and Industrial Technology Development Organization (NEDO).

References

[1] Z. Lu, D.D. MacNeil, J.R. Dahn, Electrochem. Solid-State Lett. 4 (2001) A200.
[2] D.D. MacNeil, Z. Lu, J.R. Dahn, J. Electrochem. Soc. 149 (2002) A1332.
[3] S. Jouanneau, D.D. MacNeil, Z. Lu, S.D. Beattie, G. Murphy, J.R. Dahn, J. Electrochem. Soc. 140 (2003) A1299.
[4] Z. Lu, D.D. MacNeil, J.R. Dahn, Electrochem. Solid-State Lett. 4 (2001) A191.
[5] Z. Lu, J.R. Dahn, J. Electrochem. Soc. 149 (2002) A815.
[6] Z. Lu, L.Y. Beaulieu, R.A. Donaberger, C.L. Thomas, J.R. Dahn, J. Electrochem. Soc. 149 (2002) A778.
[7] K. Numata, C. Sakaki, S. Yamanaka, Chem. Lett. 8 (1997) 725.
[8] K. Numata, C. Sakaki, S. Yamanaka, Solid State Ionics 117 (1999) 257.
[9] L. Zhang, K. Takada, N. Ohta, K. Fukuda, M. Osada, L. Wang, T. Sasaki, M. Watanabe, J. Electrochem. Soc. 152 (2005) A171.
[10] T. Ohzuku, Y. Makimura, Chem. Lett. 7 (2001) 642.
[11] T. Ohzuku, Y. Makimura, Chem. Lett. 8 (2001) 744.
[12] S.H. Kang, K. Amine, J. Power Sources 124 (2003) 533.
[13] F. Izumi, T. Ikeda, Mater. Sci. Forum 198 (2000) 321.
[14] B.J. Neudecker, R.A. Zuhr, B.S. Kwak, J.B. Bates, J. Electrochem. Soc. 145 (1998) 4148.
[15] C. Pouillerie, L. Croguennec, C. Delmas, Solid State Ionics 132 (2000) 15.
[16] R.D. Shannon, Acta Crystallogr. A 32 (1976) 751.